

Investigating the Effect of rGO Concentration on rGO-PMMA Composites Synthesized Via Solution Casting Technique

Lovepreet Singh*, Anupama Kashyap and Vishal Singh

Department of Materials Science and Engineering, National Institute of Technology, India

ISSN: 2576-8840



***Corresponding author:** Lovepreet Singh, Department of Materials Science and Engineering, National Institute of Technology, Hamirpur, Himachal Pradesh, India

Submission:  July 06, 2022

Published:  July 28, 2022

Volume 17 - Issue 3

How to cite this article: Lovepreet Singh*, Anupama Kashyap, Vishal Singh. Investigating the Effect of rGO Concentration on rGO-PMMA Composites Synthesized Via Solution Casting Technique. Res Dev Material Sci. 17(3). RDMS.000912. 2022.

DOI: [10.31031/RDMS.2022.17.000912](https://doi.org/10.31031/RDMS.2022.17.000912)

Copyright@ Lovepreet Singh. This article is distributed under the terms of the Creative Commons Attribution 4.0 International License, which permits unrestricted use and redistribution provided that the original author and source are credited.

Abstract

Reduced graphene oxide/Poly-methyl methacrylate (rGO-PMMA) based composites are successfully synthesized from solution casting technique. Earlier, Graphite Oxide (GO) was also prepared via well-known Hummers method. The effect of rGO concentration on the functional and morphological properties of PMMA is thoroughly investigated. FT-IR spectroscopy confirmed the presence of different functional groups on the surface of pure and composite material. UV-Vis and XRD helped to confirm the efficacious synthesis of GO and rGO samples. The interlayer distance in GO and rGO was calculated to be 8.6535\AA and 3.54\AA respectively. Raman spectroscopy reveals that GO and rGO has the high intensity of D and G band as compared to graphite due to disordering of a few sp^2 bonds into the sp^3 bonds. PMMA surface is comprised of plate like structure embedded with some sharp edges. SEM depicts the distortion of PMMA structure with increasing concentration of rGO load. 10% wt. rGO has the maximum effect on the structural and morphological properties of PMMA. This functional and morphological study of PMMA and rGO-PMMA composites paves the way to functionalize PMMA with other inorganic or organic substances.

Keywords: : Hummers method; Polymer composites; Raman spectroscopy; Reduced graphene oxide; Solution casting

Introduction

Composite materials are developed by integrating two distinct materials physically or chemically which gives a desired set of properties which can be modified to accomplish the requirement for different applications [1]. In polymer composites (PCs), there is combination of continuous and non-continuous reinforcements/filler. Due to versatile processing technique and reduced synthesis cost of the polymer composites, they were introduced as a structural material with upgraded properties [2]. In the previous two decades, polymer composites have attained the spotlight from ordinary composites as a result of their potential differences. There is a very wide range of polymer composites and present research is precisely focussed on reduced graphene oxide-poly (methyl meth-acrylate) (rGO-PMMA) composites [3]. PMMA is a clear polymer having amorphous crystal structure with a glass transition temperature of $\sim 100\text{ }^\circ\text{C}$. PMMA is used in many applications that demand high optical quality, requires a filler to increase strength and toughness without masking its optical properties [4]. When carbon atoms are arrayed in the hexagonal lattice after the sp^2 hybridization, an individual layer of graphene is procured [5]. A strong bonding force between the carbon atoms in graphene layer give rise to many eccentric properties like high electron mobility, high strength, high surface area, transparency and thermal conductivity [6]. Now-a-days, graphene has attracted enormous awareness in the domain of materials research as it provided numerous possibilities in emerging sectors of polymer composites. The well-known method of graphene production is to reduce Graphite Oxide (GO) to rGO [7]. This method is attractive due to its low-cost, high yield, dispersion properties of graphene in various solvents and high scalability

potential. Here, graphite is intercalated using an oxidant which lead to adsorption of functional groups containing oxygen on the graphene layer. These functional groups allow dispersion and increase the stability of GO in water [8]. Oxidation of graphite is done by the help of Hummers method which is the commonly used process to obtain graphite oxide and also used in current research work [9]. After oxidation, sonication of graphite oxide is done in water which results graphene oxide sheets which are reduced to form rGO layers. There are mainly three techniques which are used for diffusion of graphene in polymer matrix: solvent casting, melt compounding and in-situ polymerization [10-12]. In current research, rGO-PMMA composites are synthesized by solvent casting method using Dimethylformamide (DMF) as a solvent. Solution casting is a broadly used process for fabrication of graphene-based polymer composites. Usually, this method comprises three major steps: graphene is immersed in a solvent; polymer is also dispersed in the same solvent and mixed together by stirring or shears mixing, and in final step solvent is evaporated to obtain the composite material. Good dispersion of polymers and fillers depends on their compatibilities with the solvent [13]. In line with present work, Zeng et al. [14] synthesized rGO embedded PMMA composites through easy solution blending method at different wt. % of rGO such as 0.1, 0.5, 1.0, 2.0 while using Tetrahydrofuran (THF) as a solvent [14]. Kee et al. [15] premeditated the effect of preparation method on the properties of rGO-PMMA composites [15]. In the same field of work, L. Zhang et al. developed a facile route to fabricate Polypropylene(PP)/PMMA/graphene nanocomposites through the process of biaxial stretching in which graphene was oriented to in-plane direction [16]. Researchers prepared PP/PMMA/graphene nanocomposites through melt blending with three loadings of 0.5, 1.5 and 2.5 vol. % rRO. In present work, authors synthesized rGO-PMMA composites and thoroughly studied their spectroscopic and morphological characteristics with the help of different characterization techniques. To the best of author's knowledge, this is the first study which is done to reveal spectroscopic properties up to 10% rGO load in rGO-PMMA composites.

Experimental

Chemicals and reagents

Graphite powder with 99.99% purity was used as the source of GO. PMMA $[(C_5 O_2 H_8)_n]$ with high purity was employed as the matrix material in synthesized polymer composites. Sodium nitrate ($NaNO_3$, >98%) was utilized to enhance the oxidation rate. N,N-Dimethylformamide (DMF) and Sulphuric acid (H_2SO_4) were used as solvents. Potassium permanganate ($KMnO_4$, >98%) and Tri-sodium citrate ($Na_3C_6H_5O_7 \cdot 2H_2O$, 99%) were applied as oxidizing agent and reducing agents respectively. Hydrogen peroxide (H_2O_2 , 30%) was operated in removal of $KMnO_4$. DI water was used throughout the experimental process.

Instruments

Samples were centrifuged with the help of REMI R-24 centrifuge. Ultraviolet-visible (UV-Vis) spectrum was secured

Shimadzu (Model: UV-2450) UV-Vis spectrophotometer. Fourier Transform-Infrared (FT-IR) Spectrometer of Agilent Technologies (Model: L1600312) was used for FT-IR studies. X-Ray Diffraction (XRD) spectra was obtained from Powder X-ray Diffractometer of Rigaku Corporation (Model: Smart Lab 9kW). Morphological studies were done with the help of Quanta FEG 450 Scanning Electron Microscope (SEM).

Synthesis of GO

Conventional Hummers method was used for synthesis of GO. In this technique, 5gm of graphite powder was mixed with $NaNO_3$. 115ml H_2SO_4 was slowly added to the mixture and allowed to stir for 30mins at room temperature. After complete dissolution of $NaNO_3$, 15gm of $KMnO_4$ was added to the solution. The product as dense paste was obtained after stirring the mixture at room temperature for 16 hours. Then 250ml DI water was slowly added to solution with continuous stirring. 50ml of H_2O_2 was drop wise added to remove excess oxidant and to stop the reaction. The color of the solution changed to light brown upon the addition of hydrogen peroxide. Then the solution was poured off and centrifuged with the help of DI water the till its pH reached to neutral. Finally, the product was dried in a heating mantle at 600 °C and powder of GO was obtained.

Reduction of GO to rGO

25gm of $Na_3C_6H_5O_7 \cdot 2H_2O$ was added to homogeneous GO dispersion (5gm GO/250ml DI) and the mixture was stirred at 700 °C on a hot plate magnetic stirrer for 6 hours. Prediction of RGO synthesis was confirmed by changing the color of the solution (dark brown to black). The resulting solution of rGO was centrifuged and washed with DI water before drying it at 600 °C for 8 hours.

Synthesis of rGO-PMMA composites

Table 1: Different compositions of rGO-PMMA composites.

Composition Designation	Sample Name	PMMA Mass(g)	rGO Mass(g)	Mass of Composites (g)
C1	Neat PMMA	4	-	4
C2	5.0 wt.% rGO	3.8	0.2	4
C3	7.5 wt.% rGO	3.7	0.3	4
C4	10.0 wt.% rGO	3.6	0.4	4

For the preparation of rGO-PMMA composites, the required quantity of rGO was firstly dispersed in DMF and stirred for 8 hours. The desired amount of PMMA (Table 1) was also dissolved in DMF at 600 °C under constant stirring. A dispersion of RGO was then mixed to the PMMA solution and heated with vigorous stirring for 4-5 hours. Finally, the composite films were casted inside the petri dish and allowed to dry in a vacuum oven for 24

hours at 700 °C.

Results and Discussion

FT-IR analysis was done to study the different chemical groups present in pure and composite material. Spectra was recorded in the transmittance mode in the spectral range of 450-4000 cm^{-1} (Figure 1). Sample preparation was done by mixing the sample with Potassium Bromide (KBr) powder and pellets were prepared. In IR spectra of PMMA, the band observed at 758 and 1405 cm^{-1} can be attributed to CH wagging mode and -CH₃ asymmetric stretching respectively [17]. The sharp peak observed at 1643 cm^{-1} corresponds to C=O stretching vibrations [18]. The bands present at 3016 and 3618 cm^{-1} are related to C-H stretching and O- H bending vibrations in PMMA molecules [19].

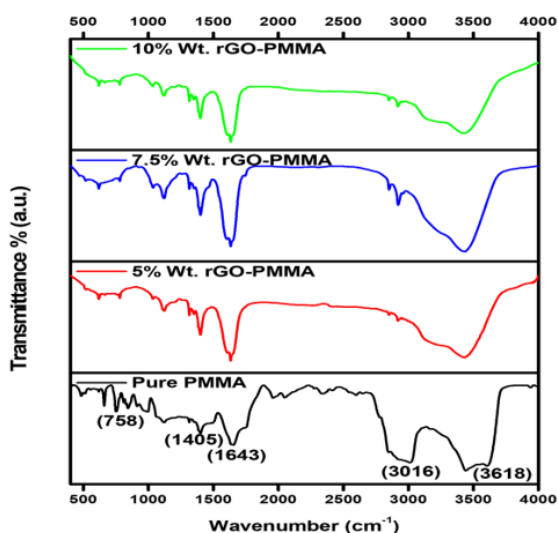


Figure 1: FT-IR spectra of Pure PMMA, 5% Wt. rGO-PMMA, 7.5% Wt. rGO-PMMA and 10% Wt. rGO-PMMA composites.

The peak present at 3016 cm^{-1} is not present in composite material due to distortion of C-H bonds during synthesis process. Another observation of IR spectrum reveals that synthesized composites with 5.0wt. % and 10.0wt. % of rGO have wider and strong peak around 3600 cm^{-1} as compared to pure PMMA due to the existence of the hydroxyl groups in rGO. Additionally, interface of RGO & PMMA might not engage chemical reaction, since new functional groups were not evidently noticed by their preparation method.

The successful preparation of GO and rGO samples was confirmed with the help of their UV- Vis spectra and XRD patterns (Figure 2). In UV-Vis spectra, GO shows a broad absorption peak in the range of 300-400nm which can be attributed to π - π^* transition of the atomic C=C bonds. And a shoulder peak in the same region was observed in rGO spectra corresponds to n - π^* transitions of C=O bonds [20]. This confirms the successful synthesis of rGO samples. In XRD spectra, GO shows an intense peak at 10.56° that corresponds to the (001) plane. After reduction of GO into rGO, there is shifting of peak to 25.11° and no evident peak of graphite

was observed due to the removal of functional groups which were added during oxidation process [21]. Interplanar distance was calculated with the help of bragg's equation: $\lambda = 2d \sin \theta$ [22]. The inter-planar distance between the layers in GO and rGO was obtained to be 8.6535 Å and 3.54Å respectively. The inter layer distance decreases on successful reduction of GO to rGO.

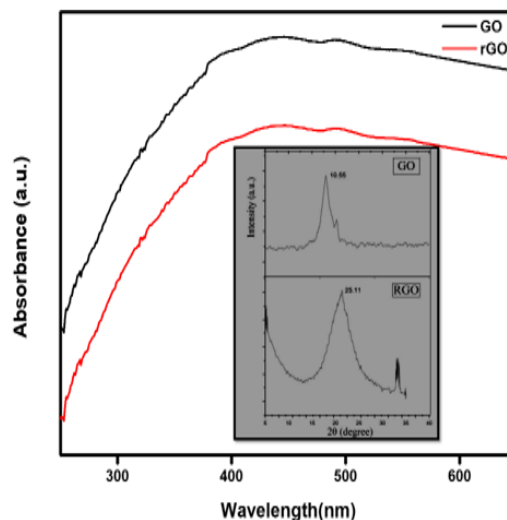


Figure 2: UV-Vis spectra of GO and rGO samples (Inset: XRD pattern of GO and rGO).

Raman spectra of samples was investigated in the spectral range of 1000-2000 cm^{-1} while using laser wavelength of 514nm (Figure 3). Raman spectroscopy is a well-known tool to characterize the carbon-based materials because they have conjugated and C=C bonds which lead to high intensity Raman peaks. Some defects are generally present in the honeycomb lattice of the carbon-based materials so there is high possibility of appearance of D bands. In graphite, GO and rGO samples, both D and G bands were present. D band peaks arrived due to out-plane vibration of the sp^2 atoms featured by structural defects [23]. G band was observed in the obtained spectra because of the sp^2 band in phase vibration of the graphite layered network. The fraction of the intensities of the D and G bands indicates toward computation of the defects in the sample. In Raman spectra of GO and rGO, the peaks of D band and G band appeared at 1353 cm^{-1} and 1587 cm^{-1} respectively [24]. It is easily observed that GO and rGO has the high intensity of D and G band as compared to graphite due to disordering of a few sp^2 bonds in the sp^3 bonds. And this disordering is created due to the presence of various functional groups after oxidation of graphite. Higher magnitude of the fraction between the intensities of D and G band implies that more binding sites are present in the sample. Table 2 summarizes that ID/IG ratio for GO is greater than the graphite, it implies that there are more defects are present in the GO. It is investigated that, microstructure is changed from graphite layered structure to exfoliated GO because multiple numbers of functional groups that contain Oxygen, were added to aromatic rings present in the base planes of graphene.

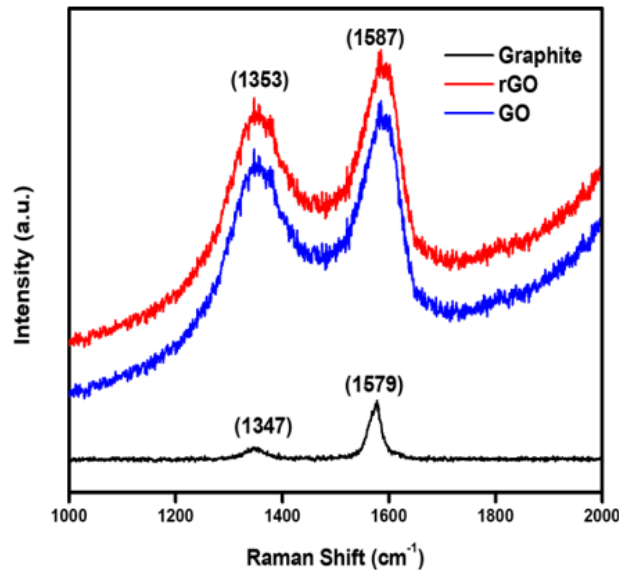


Figure 3: Raman spectra of Graphite, GO and rGO samples.

Table 2: Intensity ratio (ID/IG) of pristine graphite, GO and rGO samples.

Sample	D - band (cm-1)	G - band (cm-1)	Intensity ratio(ID/IG)
Pristine Graphite	1346	1576	0.26
GO	1350	1583	0.88
rGO	1353	1587	0.91

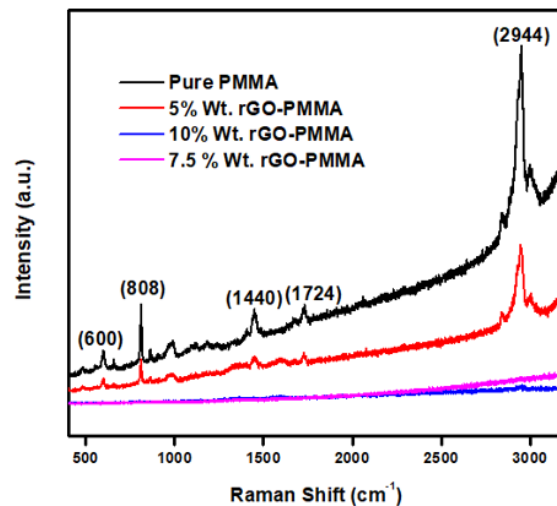


Figure 4: Raman Spectra of pure PMMA, 5% Wt. rGO-PMMA, 7.5%Wt. rGO-PMMA and 10% Wt. rGO-PMMA composites.

The Raman spectra of pure PMMA and composite material was examined in the spectral range of 450-3200 cm^{-1} (Figure 4). The most prominent band of PMMA is present at 2944 cm^{-1} which is attributed to C-H stretching vibration [25]. Another band present at 1724 cm^{-1} with low Raman intensity arises due to combination of $\nu(\text{C}=\text{C})$ and $\nu(\text{C}-\text{COO})$ modes [26]. Other Raman peaks present at 600, 800 and 1440 cm^{-1} correspond to $\nu(\text{C}-\text{COO})$, $\nu(\text{CH}_2)$ and

asymmetric (C-H) of O-CH₃ vibrational modes respectively [27].

As the load of rGO increases in PMMA matrix, traditional PMMA peaks disappear due to formation of new bonds in the composite material. A significant quenching in the Raman peaks was observed in the case of composite samples. This justifies a statement that concentration of filler materials has a great impact in alteration of functional and structural properties of polymer matrix.

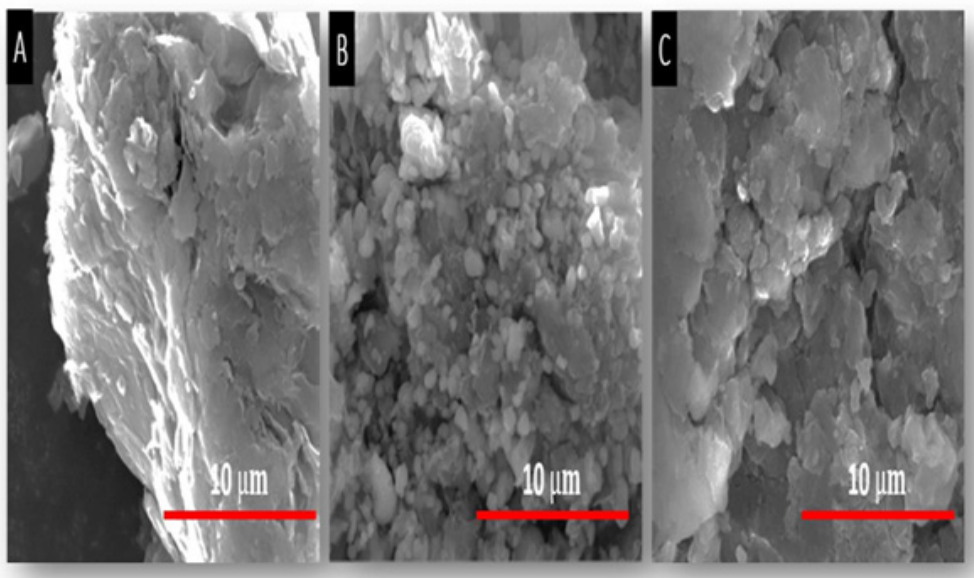


Figure 5: SEM images of (A) Graphite powder, (B) GO and (C) rGO at 10 μm scale.

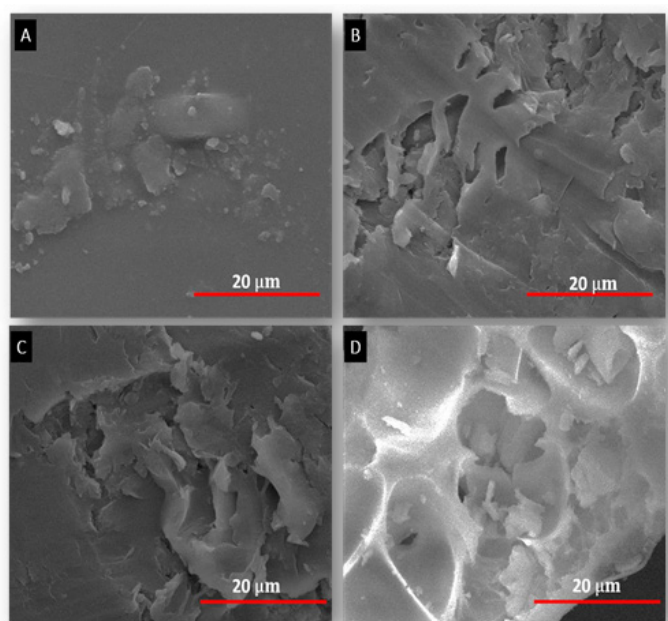


Figure 6: SEM images of (A) Pure PMMA and (B) 5% wt. rGO-PMMA, (C) 7.5% wt. rGO-PMMA and (D) 20% wt. rGO-PMMA at 20 μm scale.

Morphological studies were done with the help of SEM which reveals that Graphite has a plate like structure with some fractured surfaces (Figure 5A); [28]. The SEM images of GO shows the crumpled and layer-like flakes on its surface (Figure 5B). The flakes indicate that graphene layers got completely oxidized to GO. The SEM image of rGO thin film demonstrates that the graphene sheets were evenly separated with uniform dispersion (Figure 5C). This depicts the successful reduction of GO to rGO during synthesis process. PMMA surface is comprised of exhibited brittle fractures with some sharp edge cracks and ductile cracks (Figure 6A); [29]. When rGO was added to the PMMA matrix, a “pull out” effect was observed (Figure 6B). A strong interaction between the filler rGO and the polymer matrix was observed. The oxygen based functional groups remained bonded with the hydrogen in the Carbonyl group of PMMA. rGO can easily entangle with PMMA chains as it has wrinkled edges. As a result, a better interaction occurs between the polymer and the filler, which enhances the properties of composite material. The concentration effect of rGO on the PMMA matrix is shown in figure (Figure 6B-D). It is evident that the amount of fractures and disparity increased with the increment of rGO load in the PMMA matrix. At 10% weight of rGO-PMMA composites, there is also formation of small clusters of microscopic rods and fibres.

Present work on investigating the effect of rGO load on PMMA matrix can be extended to study the mechanical, thermal and electrical properties of pure and composite material. Limitation of current study is not able to study the effect of rGO concentration with increment of small steps (0.5g) on PMMA matrix. This research can be executed in the near future by following the same synthesis procedure as mentioned in present study.

Conclusion

Current study reports the successful preparation of rGO-PMMA composites through solvent casting method. rGO was obtained from reduction of GO which was synthesized via Conventional Hummers method. Presence of structural defects was determined by studying the D and G bands of graphite, GO and rGO. The functional groups present on the surface of pure and composite material were investigated through FT-IR and Raman spectroscopy. UV-Vis and XRD helped to confirm the efficacious devising of GO and rGO. The Interplanar distance between the layers in GO and rGO was calculated to be 8.6535 \AA and 3.54 \AA respectively. SEM revealed distortion of PMMA structure with increasing concentration of rGO load. 10% wt. rGO has the maximum effect on the structural and morphological properties of PMMA.

Acknowledgement

Authors of this paper would like to acknowledge Prof. Hiralal Murlidhar Suryawanshi (Director, National Institute of Technology, Hamirpur, India) for his constant support.

Conflict of Interest

Authors of this manuscript declare NO

References

1. Yijie X, Sun K, Ouyang J (2012) Solution-processed metallic conducting polymer films as transparent electrode of optoelectronic devices. *Advanced materials* 24(18): 2436-2440.
2. Lovepreet S, Singh V (2020) Synthesis of Au@ PANI nanocomposites by complexation method and their application as label-free chemo probe for detection of mercury ions. *Bulletin of Materials Science* 43(1): 1-10.
3. Xinyu H, William JB (2001) Synthesis and characterization of PMMA nanocomposites by suspension and emulsion polymerization. *Macromolecules* 34(10):3255-3260.
4. Khanna PK, Narendra S (2007) Light emitting CdS quantum dots in PMMA: synthesis and optical studies. *Journal of Luminescence* 127(2): 474-482.
5. Daniel RD, Sungjin P, Christopher WB, Rodney SR (2010) The chemistry of graphene oxide. *Chemical society reviews* 39(1): 228-240.
6. Jeffrey RP, Daniel RD, Christopher WB, Rodney SR (2011) Graphene-based polymer nanocomposites. *Polymer* 52(1): 5-25.
7. Sasha S, Dmitriy AD, Richard DP, Kevin AK, Alfred K, et al. (2007) Synthesis of graphene-based nanosheets via chemical reduction of exfoliated graphite oxide. *Carbon* 45(7): 1558-1565.
8. Virendra S, Daeha J, Lei Z, Soumen D, Saiful IK, et al. (2011) Graphene based materials: past, present and future. *Progress in Materials Science* 56(8): 1178-1271.
9. Zaaba NI, Foo KL, Hashim U, Tan SJ, Wei-Wen L, et al. (2017) Synthesis of graphene oxide using modified hummers method: solvent influence. *Procedia Engineering* 184: 469-477.
10. Bahrami S, Atefeh S, Hamid M, Alexander MS (2019) Electroconductive polyurethane/graphene nanocomposite for biomedical applications. *Composites Part B: Engineering* 168: 421-431.
11. Ziqing C, Xiaoyu M, Yingshuai H, Haimu Y, Lishan C, et al. (2015) Reinforcing polyamide 1212 with graphene oxide via a two-step melt compounding process. *Composites Part A: Applied Science and Manufacturing* 69: 115-123.
12. Saswata B, Tapas K, Elias U, Nam-Hoon K, Alan KTL, et al. (2010) In-situ synthesis and characterization of electrically conductive polypyrrole/graphene nanocomposites. *Polymer* 51.25 (2010): 5921-5928.
13. Lovepreet S, Vishal S (2021) Study of structural and functional properties of graphene/polyaniline nanocomposites synthesized via in situ polymerization. *Advances in Mechanical Engineering*. Springer, Singapore, pp. 1-10.
14. Xiaopeng Z, Jingjing Y, Wenxia Y (2012) Preparation of a poly (methyl methacrylate)-reduced graphene oxide composite with enhanced properties by a solution blending method. *European Polymer Journal* 48(10): 1674-1682.
15. Shin YK, Yamuna M, Kok SO, Koon CL (2017) Effect of preparation methods on the tensile, morphology and solar energy conversion efficiency of RGO/PMMA nanocomposites. *Polymers* 9(6): 230.
16. Feng Y, Xinye L, Liang Z, Dongrui W, Chang YS, et al. (2017) Polypropylene/poly (methyl methacrylate)/graphene composites with high electrical resistivity anisotropy via sequential biaxial stretching. *RSC advances* 7(10): 6170-6178.
17. Rajendraz S, Uma T (2000) Lithium-ion conduction in PVC-LiBF₄ electrolytes gelled with PMMA. *Journal of Power Sources* 88(2): 282-285.
18. Ramesh S, Koay HL, Kumutha K, Arof AK (2007) FTIR studies of PVC/PMMA blend based polymer electrolytes. *Spectrochimica Acta Part A: Molecular and Biomolecular Spectroscopy* 66(4-5): 1237-1242.

19. Huszank R, Szilágyi E, Szoboszlai Z, Szikszai Z (2019) Investigation of chemical changes in PMMA induced by 1.6 MeV He⁺ irradiation by ion beam analytical methods (RBS-ERDA) and infrared spectroscopy (ATR-FTIR). *Nuclear Instruments and Methods in Physics Research Section B: Beam Interactions with Materials and Atoms* 450: 364-368.
20. Adere TH, Delele WA (2019) Synthesis and characterization of reduced graphene oxide (rGO) started from graphene oxide (GO) using the tour method with different parameters. *Advances in Materials Science and Engineering*.
21. Tapas K, Sambhu B, Dahu Y, Nam HK, Saswata B, et al. (2010) Recent advances in graphene-based polymer composites. *Progress in polymer science* 35(11): 1350-1375.
22. Spong A, Phummanee S, Somwangthanaroj A (2007) Effect of clay on mechanical and gas barrier properties of blown film LDPE/clay nanocomposites. *Journal of Applied Polymer Science* 106(4): 2210-2217.
23. Sharma N, Vikas S, Yachana J, Mitlesh K, Ragini G, et al. (2017) Synthesis and characterization of graphene oxide (GO) and reduced graphene oxide (rGO) for gas sensing application. *Macromolecular Symposia* 376(1).
24. Young LA, Kihyuk Y, Nguyen DA, Chulho P, Seung ML, et al. (2021) Raman study of D* band in graphene oxide and its correlation with reduction. *Applied surface science* 536: 147990.
25. Willis HA, Veronica JIZ, Parick JH (1969) The laser-Raman and infra-red spectra of poly (methyl methacrylate). *Polymer* 10: 737-746.
26. Thomas KJ, Sheeba M, Nampoorei VPN, Vallabhan CPG, Radhakrishnan P, et al. (2008) Raman spectra of polymethyl methacrylate optical fibres excited by a 532 nm diode pumped solid state laser. *Journal of Optics a: Pure and Applied Optics* 10(5): 055303.
27. Xingsheng X, Ming H, Zhang Q, Zhang Y (2002) Properties of Raman spectra and laser-induced birefringence in polymethyl methacrylate optical fibres. *Journal of Optics A: Pure and Applied Optics* 4.3 (2002): 237.
28. Long L, Weixing Z, Ling Y, Ximing Z, Wen F (2021) Etching characteristic of graphite and metal substrates by hydrocarbon plasma in closed cavity. *Plasma Chemistry and Plasma Processing* 41(2): 691-705.
29. Zhang Y, Yin-yan C, Li H, Zhi-guo C, Li-juan S, et al. (2017) The antifungal effects and mechanical properties of silver bromide/cationic polymer nano-composite-modified Poly-methyl methacrylate-based dental resin. *Scientific Reports* 7(1): 1-13.